Syntheses, Structures Tuned by 4,4′-Bipyridine and Magnetic Properties of a Series of Transition Metal Compounds Containing o-Carboxylphenoxyacetate Acid

ARTICLE *in* CRYSTAL GROWTH & DESIGN · JANUARY 2012

Impact Factor: 4.89 · DOI: 10.1021/cg201197k

9 AUTHORS, INCLUDING:

Bin Zhao
Nankai University
126 PUBLICATIONS **5,384** CITATIONS
SEE PROFILE

Wei Shi
Nankai University
153 PUBLICATIONS **6,224** CITATIONS
SEE PROFILE

Peng Cheng
Nagoya Gakuin University
367 PUBLICATIONS **8,064** CITATIONS
SEE PROFILE

CRYSTAL GROWTH & DESIGN

Article

pubs.acs.org/crystal

Syntheses, Structures Tuned by 4,4′-Bipyridine and Magnetic Properties of a Series of Transition Metal Compounds Containing *o*-Carboxylphenoxyacetate Acid

Zhi Chen,[†] Dong-Liang Gao,[†] Chun-Hua Diao,[‡] Yue Liu,[†] Jia Ren,[†] Ji Chen,[†] Bin Zhao,*[,†] Wei Shi,[†] and Peng Cheng[†]

[†]Department of Chemistry, Key Laboratory of Advanced Energy Material Chemistry, MOE, and TKL of Metal and Molecule Based Material Chemistry, Nankai University, Tianjin 300071, P. R. China

[‡]College of Sciences, Tianjin University of Science and Technology, Tianjin 300222, P. R. China

Supporting Information

ABSTRACT: Nine compounds based on *o*-carboxylphenoxyacetate acid (H_2OCPA) ligand: $[Cu(OCPA)(4,4'\text{-bipy})_{0.5}]_n$ (**1**), $\{[Cu_2(OCPA)_2(4,4'\text{-bipy})_2(H_2O)]\cdot H_2O\}_n$ (**2**), $[Co_2(OCPA)_2(4,4'\text{-bipy})(H_2O)_4]$ (**3**), $\{[Co(OCPA)(4,4'\text{-bipy})_{0.5}(H_2O)]\cdot H_2O\}_n$ (**4**), $\{[Co(OCPA)(4,4'\text{-bipy})_{1.5}]\cdot 0.5H_2O\}_n$ (**5**), $[Ni_2(OCPA)_2(4,4'\text{-bipy})(H_2O)_4]$ (**6**), $\{[Ni(OCPA)(4,4'\text{-bipy})_{1.5}]\cdot 2H_2O\}_n$ (**7**), $\{[Zn(OCPA)(4,4'\text{-bipy})_{0.5}(H_2O)]\cdot H_2O\}_n$ (**8**), and $[Mn(OCPA)(H_2O)]_n$ (**9**) (4,4′-bipy = 4,4′-bipyridine) were synthesized by hydrothermal methods. The results of structural analyses reveal that the giant structural divergence of the compounds with same metal ions mainly originated from the different amounts of 4,4′-bipy used in syntheses. For Cu-containing compounds, the structural divergences are from one-dimensional (1D) chain **1** to two-dimensional (2D) network **2**; for Co, through binuclear **3** to 1D ladder-like **4**, and to another different 1D ladder-like chain **5**; for Ni, from binuclear **6** to 1D chain **7**. But for Zn and Mn, 1D chain **8** and 2D network **9** are obtained with the presence of excess 4,4′-bipy. Compound **9** crystallizes in chiral space group $P2_1$ with a second harmonic generation (SHG) efficiency of 0.8 times that of urea. The magnetic studies show that compounds **1** and **9** have antiferromagnetic coupling between the adjacent metallic ions. Compound **4** is a weak ferromagnet based on antiferromagnetic interaction and spin canting. Both the bifurcation temperature of the field-cooled (FC) and zero-field-cooled (ZFC) and the peaks of the real χ_M' and the imaginary χ_M'' parts of alternating current (AC) magnetic susceptibilities are observed at 2.2 K, indicated that the critical temperature T_c is 2.2 K. A very little hysteresis loop is observed with a small coercive field of 20 Oe.

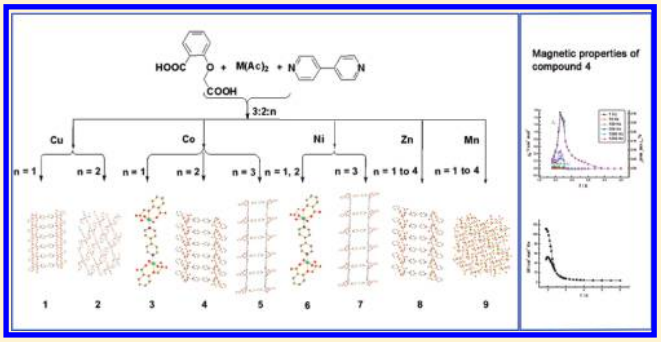

INTRODUCTION

The diversity of molecular structures and weak interactions provides materials abundance characteristics and functions, such as magnetic,[1] luminescence,[2] chemical sensing,[3] catalytic,[4] nonlinear,[5] electro-active,[6] molecular-based devices,[7] and multifunctional materials.[8] In the research area of magnetic functional materials, spin canting belongs to a very interesting magnetic phenomenon.[9−14] Because of the antisymmetric exchange and strong single-ion magnetic anisotropy, the spin arrangements on two sublattices of an antiferromagnet are neither completely parallel nor antiparallel, but are non-collinear, resulting in a spin canting magnetic phenomenon. For the antiferromagnetic coupling system with the same spin carrier, spin canting may cause no compensation of the magnetic moments and provokes weak ferromagnetism.[9] Up to now, the canted systems such as Co^{II},[10] Fe^{II},[11] Mn^{II},[12] Mn^{III},[12] Ni^{II},[13] and Re^{IV}[14] have been documented. However, more examples and magnetic studies associated with spin canting should be provided and are also indispensable for the exploration of the magneto-structural relationship, because this is an effective pathway to controllably prepare desired molecule-based magnets in the future.[12d,15]

On the other hand, from the crystal-engineering point of view, the realization of controllable structures with desired physical properties are a great challenge.[16] Indeed, many subtle factors, including reaction temperature, the ratio of reagents, solvents, pH value, anions, the multiformity of ligands, the coordination nature of metal ions, and so on, may influence the molecules assembly.[17] Thereby, the investigation on assembly rules of molecules under certain specific conditions becomes very important. In this contribution, the effect of different amounts of 4,4′-bipyridine (4,4′-bipy) on the structure assembly was systematically explored.

Received: September 13, 2011
Revised: December 19, 2011
Published: January 31, 2012

   dx.doi.org/10.1021/cg201197k | *Cryst. Growth Des.* 2012, 12, 1201−1211

Table 1. Crystallographic Data for 1−9

	1	2	3	4	5	6	7	8	9
empirical formula	$C_{14}H_{10}CuNO_5$	$C_{38}H_{32}Cu_2N_4O_{12}$	$C_{28}H_{28}Co_2N_2O_{14}$	$C_{14}H_{14}CoNO_7$	$C_{24}H_{19}CoN_3O_{5.50}$	$C_{28}H_{28}N_2Ni_2O_{14}$	$C_{24}H_{22}N_3NiO_7$	$C_{14}H_{14}NO_7Zn$	$C_9H_8MnO_6$
formula weight	335.78	863.78	734.38	367.19	496.35	733.90	523.14	373.63	267.09
T/K	293(2)	293(2)	293(2)	293(2)	293(2)	293(2)	293(2)	293(2)	293(2)
λ/Å	0.71073	0.71073	0.71073	0.71073	0.71073	0.71073	0.71073	0.71073	0.71073
cryst system	monoclinic	triclinic	monoclinic	monoclinic	monoclinic	triclinic	monoclinic	monoclinic	monoclinic
space group	$P2_1/c$	$P\bar{1}$	$P2_1/c$	$C2/c$	$P2_1/c$	$P\bar{1}$	$P2_1/c$	$C2/c$	$P2_1$
a/Å	7.485(3)	7.5343(15)	9.7351(10)	29.703(4)	11.450(2)	6.5870(13)	11.370(2)	29.479(3)	5.2040(11)
b/Å	31.617(13)	15.432(3)	23.513(3)	5.1857(7)	14.170(3)	9.866(2)	14.137(3)	5.1262(5)	9.634(2)
c/Å	5.169(2)	16.814(3)	6.5060(8)	19.504(3)	15.695(3)	11.756(2)	15.113(3)	19.3570(17)	9.777(2)
α/deg	90	116.35(3)	90	90	90	97.88(3)	90	90	90
β/deg	106.19(2)	92.04(3)	107.709(7)	109.106(4)	110.06(3)	105.16(3)	107.63(3)	109.018(3)	91.737(4)
γ/deg	90	90.63(3)	90	90	90	102.98(3)	90	90	90
V/Å^3	1174.7(8)	1749.9(6)	1418.7(3)	2838.7(7)	2392.0(8)	702.8(2)	2315.1(8)	2765.4(4)	489.95(18)
Z	4	2	2	8	4	1	4	8	2
Dcalcd (g·cm^{-3})	1.899	1.639	1.719	1.718	1.378	1.734	1.501	1.795	1.810
μ/mm^{-1}	1.883	1.290	1.248	1.248	0.758	1.419	0.889	1.816	1.357
F(000)	680	884	752	1504	1020	378	1084	1528	270
GOF	1.149	1.004	1.140	1.125	1.104	0.975	1.046	1.103	1.131
R_1 [$I > 2\sigma(I)$]	0.0409	0.0362	0.0463	0.0413	0.0825	0.0453	0.0718	0.0366	0.0179
wR_2	0.0969	0.0885	0.0866	0.0810	0.2092	0.0897	0.1580	0.0893	0.0439
R_1 (all data)	0.0492	0.0526	0.0690	0.0455	0.1078	0.0706	0.0957	0.0411	0.0183
wR_2	0.1004	0.0956	0.0933	0.0828	0.2290	0.0965	0.1712	0.0922	0.0441

dx.doi.org/10.1021/cg201197k | Cryst. Growth Des. 2012, 12, 1201−1211

It was well-known that the selection of organic ligands plays a crucial role in the rational design and construction of coordination polymers, and polycarboxylate-type ligands have been widely employed as linkers of metal ions to obtain unique coordination polymers with interesting magnetic properties.[18] In our work, we choose *o*-carboxylphenoxyacetate acid (H_2OCPA) as a ligand based on the following aspects: (1) the rigidity of the benzene ring and flexibility of substituent groups may cause the generation of diversiform coordination modes; (2) it is an easily coordinated ligand by chelating metal ions with an ether oxygen atom and two carboxyl oxygen atoms, supported by reported results.[19] Additionally, 4,4′-bipy is a neutral organic pillared bridging ligand and frequently used to connect the transition metal nodes to lengthen their distances in the synthesis of mixed-ligand metal−organic frameworks.[20] It also can be a very good organic base which influences the structure and property of a compound. In particular, when the metal nodes have coordinated water molecules, the replacement of 4,4′-bipy may give rise to a high dimensional compound.

In this work, by using ligand H_2OCPA and tuning the amount of 4,4′-bipy, a series of coordination compounds $[Cu(OCPA)(4,4'\text{-bipy})_{0.5}]_n$ (**1**), $\{[Cu_2(OCPA)_2(4,4'\text{-bipy})_2(H_2O)]\cdot H_2O\}_n$ (**2**), $[Co_2(OCPA)_2(4,4'\text{-bipy})(H_2O)_4]$ (**3**), $\{[Co(OCPA)(4,4'\text{-bipy})_{0.5}(H_2O)]\cdot H_2O\}_n$ (**4**), $\{[Co(OCPA)(4,4'\text{-bipy})_{1.5}]\cdot 0.5H_2O\}_n$ (**5**), $[Ni_2(OCPA)_2(4,4'\text{-bipy})(H_2O)_4]$ (**6**), $\{[Ni(OCPA)(4,4'\text{-bipy})_{1.5}]\cdot 2H_2O\}_n$ (**7**), $\{[Zn(OCPA)(4,4'\text{-bipy})_{0.5}(H_2O)]\cdot H_2O\}_n$ (**8**), and $[Mn(OCPA)(H_2O)]_n$ (**9**) were prepared by hydrothermal methods. The significant structure differences from dinuclear to one-dimensional (1D) chains to two-dimensional (2D) networks were given through changing the 4,4′-bipy amount. A second-order nonlinear optical property measurement indicated that compound **9** with chiral space group $P2_1$ exhibited second harmonic generation (SHG) efficiency about 0.8 times that of urea. The study of magnetic properties showed that compound **4** was a weak ferromagnet based on antiferromagnetic interaction and spin canting with a critical temperature of 2.2 K.

EXPERIMENTAL SECTION

Materials and General Characterization. All chemicals are analytical grade. Analyses for C, H, and N were carried out on a Perkin-Elmer elemental analyzer. The Fourier transform infrared (FT-IR) spectra were measured with a Bruker Tensor 27 spectrophotometer on KBr disks. The magnetic properties were measured on a Quantum Design MPMS-XL7 and a PPMS-9 ACMS magnetometer. Diamagnetic corrections were made with Pascal's constants for all the constituent atoms. Powder X-ray diffraction measurements were recorded on a D/Max-2500 X-ray diffractometer using Cu Kα radiation.

X-ray Diffraction Analyses. Crystallographic data of **1**, **3**, **4**, **8**, and **9** were collected with a SCX-MINI CCD area detector, and data of **2**, **5**, **6**, and **7** were collected with a Bruker SMART 1000 CCD area detector. Both detectors were equipped with graphite monochromatic Mo Kα radiation (λ = 0.71073 Å). The structures were solved by the direct method and refined by the full-matrix least-squares method on F^2 with anisotropic thermal parameters for all non-hydrogen atoms.[21,22] Hydrogen atoms were located geometrically and refined isotropically. It should be noted that the O1 atom of the $OCPA^{2-}$ ligand in compound **5** and water molecules in compound **7** were treated by disorder, and these atoms were refined anisotropically with the application of restraints on interatomic distances and thermal parameters (DFIX, ISOR, and EADP instructions in SHELXL). The most disagreeable reflections of the two compounds were also omitted. Crystallographic data for the nine compounds are listed in Table 1.

Preparation of Compounds. $[Cu(OCPA)(4,4'\text{-bipy})_{0.5}]_n$ (**1**): A mixture of H_2OCPA (0.3 mmol, 57.6 mg), $Cu(Ac)_2\cdot 6H_2O$ (0.2 mmol, 57.9 mg), 4,4′-bipy (0.1 mmol, 19.2 mg), and H_2O (8 mL) was placed in a 20 mL autoclave and then heated at 120 °C for three days and then cooled to room temperature at the speed of 1.5 °C/h. The dark green plate crystals were obtained in 34% yield based on Cu. Elemental analysis, Calc: C, 50.08; H, 3.00; N 4.17. Found: C, 49.80; H, 3.26; N, 4.19. IR (KBr, cm^{-1}): 3410 s, 3079 m, 2982 m, 1675 s, 1588 s, 1548 s, 1483 w, 1455 w,1395 s, 1370 m, 1340 w, 1234 m, 1207 m, 1167 w, 1101 w, 1082 w, 1048 w, 1003 m, 949 w, 873 m, 835 s, 773 s, 733 w, 697 w, 669 w, 646 w.

*$\{[Cu_2(OCPA)_2(4,4'\text{-bipy})_2(H_2O)]\cdot H_2O\}_n$ (**2**).* The preparation of **2** was similar to that of **1** except that 0.2 mmol of 4,4′-bipy (38.4 mg) was added. The dark blue block crystals were obtained in 90% yield based on Cu. Elemental analysis, Calc: C, 52.84; H, 3.73; N 6.49. Found: C, 52.42; H, 3.88; N, 6.57. IR (KBr, cm^{-1}): 3452 m, 1611 s, 1489 m, 1457 w, 1401 s, 1344 w, 1252 w, 1221 s, 1109 m, 1076 w, 1051 w, 818 s, 766 s, 728 w, 646 m.

*$[Co_2(OCPA)_2(4,4'\text{-bipy})(H_2O)_4]$ (**3**).* The preparation of **3** was similar to that of **1** except that $Co(Ac)_2\cdot 6H_2O$ (0.2 mmol, 57.0 mg) was added, instead of $Cu(Ac)_2\cdot 6H_2O$. The light brown block crystals were obtained in 62% yield based on Co. Elemental analysis, Calc: C, 45.79; H, 3.84; N 3.81. Found: C, 45.80; H, 4.09; N, 3.94. IR (KBr, cm^{-1}): 3382 m, 3109 m, 1603 s, 1560 m, 1479 m, 1436 s, 1417 s, 1357 s, 1271 w, 1210 s, 1166 m, 1153 m, 1096 m, 1053 w, 1028 s, 952 m, 871 m, 834 m, 812 s, 768 s, 697 m, 657 m, 639 m.

*$\{[Co(OCPA)(4,4'\text{-bipy})_{0.5}(H_2O)]\cdot H_2O\}_n$ (**4**).* The preparation of **4** was similar to that of **3** except that 0.2 mmol of 4,4′-bipy (38.4 mg) was added. The violet block crystals were obtained in 50% yield based on Co. Elemental analysis, Calc: C, 45.79; H, 3.84; N 3.81. Found: C, 45.04; H, 3.64; N, 3.77. IR (KBr, cm^{-1}): 3398 s, 1608 s, 1488 m, 1411 s, 1352 m, 1281 m, 1248 w, 1212 s, 1172 s, 1101 s, 1070 m, 1032 s, 947 s, 838 w, 865 s, 829 w, 811 s, 762 s, 721 m, 657 m, 637 m.

*$\{[Co(OCPA)(4,4'\text{-bipy})_{1.5}]\cdot 0.5H_2O\}_n$ (**5**).* The preparation of **5** was similar to that of **3** except that 0.3 mmol of 4,4′-bipy (57.7 mg) was added. The dark orange needle crystals were obtained in 41% yield based on Co. Elemental analysis, Calc: C, 58.07; H, 3.86; N 8.46. Found: C, 57.12; H, 4.19; N, 8.37. IR (KBr, cm^{-1}): 3423 s, 1605 s, 1561 w, 1488 w, 1410 s, 1217 m, 1101 w, 1067 w, 866 w, 812 m, 752 w, 630 w.

*$[Ni_2(OCPA)_2(4,4'\text{-bipy})(H_2O)_4]$ (**6**).* The preparation of **6** was similar to that of **1** except that $Ni(Ac)_2\cdot 6H_2O$ (0.2 mmol, 57.0 mg) was added, instead of $Cu(Ac)_2\cdot 6H_2O$. The green block crystals were obtained in 88% yield based on Ni. Elemental analysis, Calc: C, 45.82; H, 3.84; N 3.82. Found: C, 45.22; H, 3.85; N, 3.89. IR (KBr, cm^{-1}): 3337 s, 1621 s, 1562 s, 1479 m, 1418 s, 1368 s, 1342 m, 1225 m, 1207 s, 1164 m, 1096 m, 1069 m, 1049 w, 1027 s, 947 m, 871 m, 837 m, 808 s, 773 s, 697 w, 659 w, 641 w.

*$\{[Ni(OCPA)(4,4'\text{-bipy})_{1.5}]\cdot 2H_2O\}_n$ (**7**).* The preparation of **7** was similar to that of **6** except that 0.3 mmol of 4,4′-bipy (57.7 mg) was added. The blue needle crystals were obtained in 57% yield based on Ni. Elemental analysis, Calc: C, 55.10; H, 4.24; N 8.03. Found: C, 55.32; H, 4.29; N, 8.17. IR (KBr, cm^{-1}): 3460 s, 1613 s, 1567 w, 1536 w, 1481 m, 1408 s, 1363 s, 1218 s, 1205 s, 1165 w, 1097 w, 1069 m, 1046 w, 1024 w, 943 w, 868 m, 834 s, 815 m, 750 s, 735 m, 696 w, 633 s.

*$\{[Zn(OCPA)(4,4'\text{-bipy})_{0.5}(H_2O)]\cdot H_2O\}_n$ (**8**).* The preparation of **8** was similar to that of **7** except that $Zn(Ac)_2\cdot 6H_2O$ (0.2 mmol, 58.3 mg) was added, instead of $Ni(Ac)_2\cdot 6H_2O$. The colorless block crystals were obtained in 82% yield based on Zn. Elemental analysis, Calc: C, 45.00; H, 3.78; N 3.75. Found: C, 45.04; H, 3.64; N, 3.87. IR (KBr, cm^{-1}): 3419 m, 1609 s, 1550 s, 1490 m, 1435 m, 1411 s, 1352 m, 1280 w, 1249 w, 1221 s, 1171 m, 1102 m, 1071 m, 1040 m, 949 w, 883 w, 865 m, 829 w, 812 m, 762 s, 726 w, 657 w, 639 m.

*$[Mn(OCPA)(H_2O)]_n$ (**9**).* The preparation of **9** was similar to that of **8** except that $Mn(Ac)_2\cdot 6H_2O$ (0.2 mmol, 56.2 mg) was used, instead of $Zn(Ac)_2\cdot 6H_2O$. The colorless needle crystals were obtained in 75% yield based on Mn. Elemental analysis, Calc: C, 40.47; H, 3.02. Found: C, 40.68; H, 3.18. IR (KBr, cm^{-1}): 3375 m, 1675 m, 1633 s, 1590 s, 1541 s, 1486 m, 1450 s, 1423 s, 1395 s, 1350 m, 1280 w, 1214 s, 1172

dx.doi.org/10.1021/cg201197k | *Cryst. Growth Des.* 2012, 12, 1201−1211

m, 1107 m, 1039 m, 954 m, 864 m, 827 m, 768 s, 706 m, 615 w, 598 w, 537 w, 517 w.

RESULT AND DISCUSSION

Syntheses. Compounds **1**−**7** were successfully obtained by changing the 4,4′-bipy amount, as shown in Scheme 1. The molar ratio of H_2OCPA ligand, metal salts, and 4,4′-bipy in preparing these compounds may be considered as 3:2:*n*, and for the same metal system, different *n* will result in different structures. For example, for Cu when *n* = 1, the 1D chain **1** was obtained, while *n* = 2, the 2D network **2** was formed; for Co, as *n* = 1, 2, and 3, corresponding binuclear **3**, 1D chain **4** and another 1D chain **5** were obtained, respectively; for Ni, binuclear **6** (*n* = 1 and 2) and 1D chain **7** (*n* = 3) were also obtained. But for the Zn and Mn system, 1D chain **8** (Zn) and 2D network **9** (Mn) still remained unchanged even after altering the amount of 4,4′-bipy from 1 to 4 equiv.

Scheme 1. Synthetic Strategy of Compounds 1−9[a]

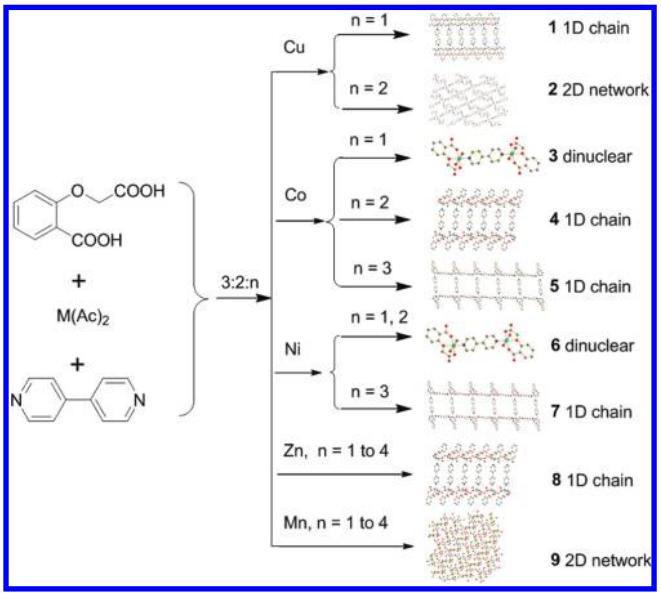

[a] 3:2:*n* means the molar ratio of H_2OCPA/metal salt/4,4′-bipy.

Description of Crystal Structures. [Cu(OCPA)(4,4′-bipy)$_{0.5}$]$_n$ (1). The compound **1** crystallizes in the monoclinic system with space group $P2_1/c$. Its asymmetric unit consists of one $OCPA^{2-}$, half a 4,4′-bipy, and one Cu(II) ion (Figure 1). The pentacoordinated sphere of the Cu(II) ion is completed by one nitrogen atom of 4,4′-bipy and four oxygen atoms from two $OCPA^{2-}$, resulting in a distorted CuO_4N rectangular pyramid, in which the apical position is occupied by O4A from adjacent ligand. The Cu−O bond lengths range from 1.873 to 2.337 Å, and the Cu−N bond distance is 1.990 Å. $OCPA^{2-}$ as a tridentate (O1, O3, and O5 atoms) ligand chelates to the Cu1 center. Two crystallographically equal Cu(II) centers are bridged by one 4,4′-bipy molecule into a centrosymmetric binuclear unit [Cu_2(OCPA)$_2$(4,4′-bipy)], and then such units are further bridged by O4 atoms of $OCPA^{2-}$ into an infinite 1D ladder-like chain (Figure 2).

{[Cu$_2$(OCPA)$_2$(4,4′-bipy)$_2$(H$_2$O)]·H$_2$O}$_n$ (2). The structure of **2** belongs to the triclinic system with space group $P\bar{1}$. There are two crystallographically independent Cu(II) ions, two $OCPA^{2-}$, two 4,4′-bipy molecules, one coordinated water molecule, and one lattice water molecule in an asymmetric unit

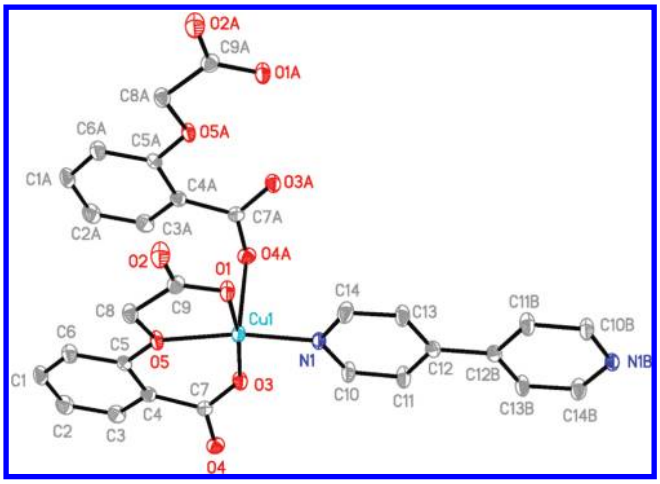

Figure 1. The molecular structure of compound **1**.

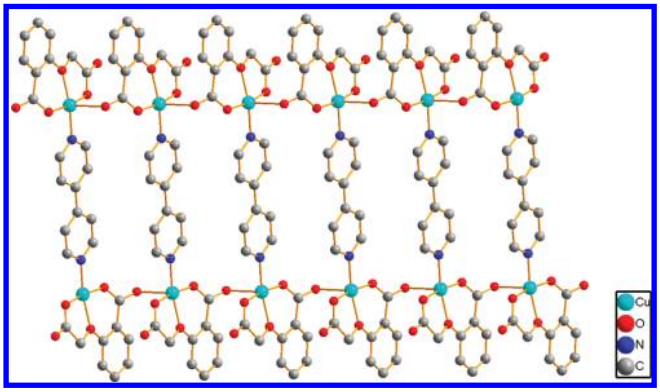

Figure 2. The 1D structure of compound **1**.

(Figure 3). Two oxygen atoms (O3 and O6) of two $OCPA^{2-}$ anions, and two nitrogen atoms (N3 and N4) from two different 4,4′-bipy ligands, form the CuN_2O_2 tetragonal geometry configuration. Additionally, two oxygen atoms O4 and O5 have weak coordination bonds to Cu1 with lengths of 2.680 and 2.595 Å, respectively. For Cu2 atom, two oxygen atoms (O2 and O8A) from two carboxylate groups, two nitrogen atoms (N2A and N1A) from two different 4,4′-bipy ligands, and one water molecule complete a rectangular pyramid. The Cu−O bond lengths of compound **2** range

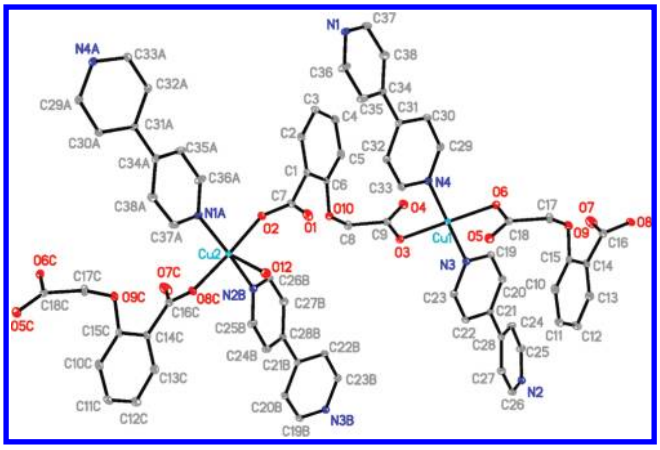

Figure 3. The molecular structure of compound **2**.

dx.doi.org/10.1021/cg201197k | *Cryst. Growth Des.* 2012, 12, 1201−1211

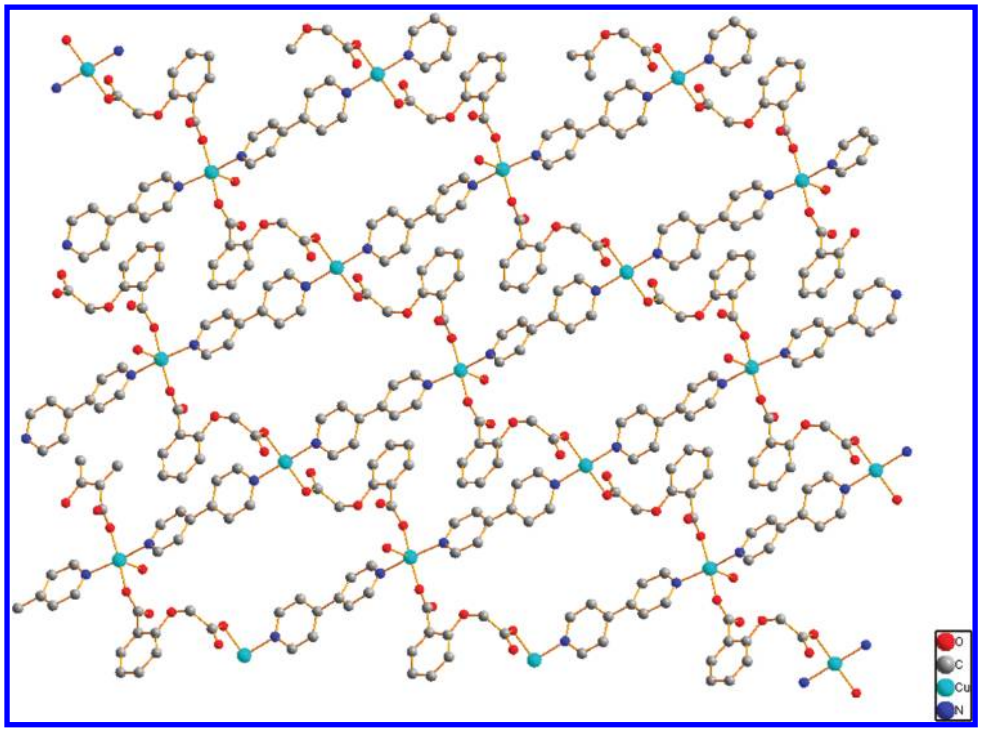

Figure 4. The 2D structure of compound **2**.

from 1.930 to 2.339 Å, and the Cu−N bond lengths fall in the range of 2.002−2.032 Å. $OCPA^{2-}$ as didentate ligand linked the Cu(II) center into a 1D chain. The adjacent 1D chains are further bridged by 4,4′-bipy ligands into a 2D lattice (Figure 4).

$[Co_2(OCPA)_2(4,4'\text{-bipy})(H_2O)_4]$ (3) and $[Ni_2(OCPA)_2(4,4'\text{-bipy})(H_2O)_4]$ (6). Single crystal X-ray diffraction results reveal that compounds **3** and **6** have a similar binuclear structure (Figure 5), although they crystallize

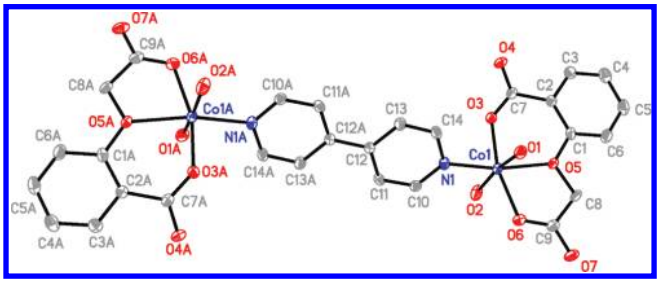

Figure 5. The molecular structure of compound **3**.

in different space groups of $P2_1/c$ and $P\bar{1}$, respectively. In **3**, The Co(II) ion is in an octahedral coordination sphere, in which the equatorial positions are occupied by three oxygen atoms from one $OCPA^{2-}$ ligand and one nitrogen atom from the 4,4′-bipy ligand. The axial positions are occupied by two water molecules. The Co−O bond lengths range from 1.994 to 2.183 Å, and the Co−N bond distance is 2.090 Å. Two Co(II) ions are connected by 4,4′-bipy to generate a binuclear motif. In **6**, The Ni−O bond lengths range from 1.988 to 2.092 Å, and the Ni−N bond distance is 2.037 Å. The binuclear motifs in both **3** and **6** are further assembled into a three-dimensional (3D) framework through four types of hydrogen bonds along the *b* and *c* direction (for hydrogen bond tables of **3** and **6**, see Supporting Information, Tables 2 and 3). All hydrogen bonds involve the coordinated water molecules and the carboxylate oxygen atoms. In compound **6**, all molecules array parallelly, while in compound **3**, they array with an angle of 53.88° in the plane (110). Thus, the different packing modes result in the different space groups of **3** and **6** (see Supporting Information).

$\{[Co(OCPA)(4,4'\text{-bipy})_{0.5}(H_2O)]\cdot H_2O\}_n$ (4) and $\{[Zn(OCPA)(4,4'\text{-bipy})_{0.5}(H_2O)]\cdot H_2O\}_n$ (8). The structures of **4** and **8** are isomorphous with space group *C*2/*c*, and the structure of **4** as an example was described here. The asymmetric unit of compound **4** consists of one $OCPA^{2-}$, half a 4,4′-bipy, one coordinated water molecule, and one Co(II) ion (Figure 6). The six-coordinated sphere of the

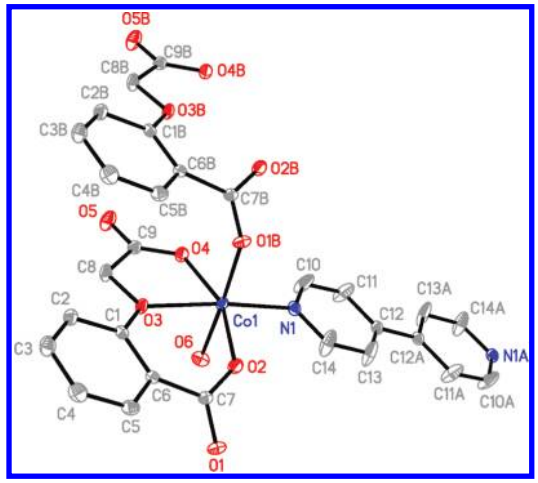

Figure 6. The molecular structure of compound **4**.

Co(II) ion is completed by one nitrogen atom of 4,4′-bipy, four oxygen atoms from two $OCPA^{2-}$, and one coordinated water molecule, resulting in a distorted CoO_5N octahedron. The axial position is occupied by O1A from an adjacent ligand and one coordinated water molecule. The Co−O bond lengths range

dx.doi.org/10.1021/cg201197k | *Cryst. Growth Des.* 2012, 12, 1201−1211

from 2.015 to 2.221 Å, and the Co−N bond distance is 2.122 Å. In **8**, The Zn−O bond lengths range from 1.9736 to 2.2776 Å, and the Zn−N bond distance is 2.074 Å. The $OCPA^{2-}$ ligand employs a tridentate (O2, ether O3 and O4 atoms) mode chelated to the Co1 center like that chelated to Cu1 in compound **1**. Adjacent Co(II) ions are bridged by carboxyl groups into 1D chains, and then two adjacent chains are further linked by 4,4′-bipy molecules into an infinite 1D ladder-like chain (Figure 7).

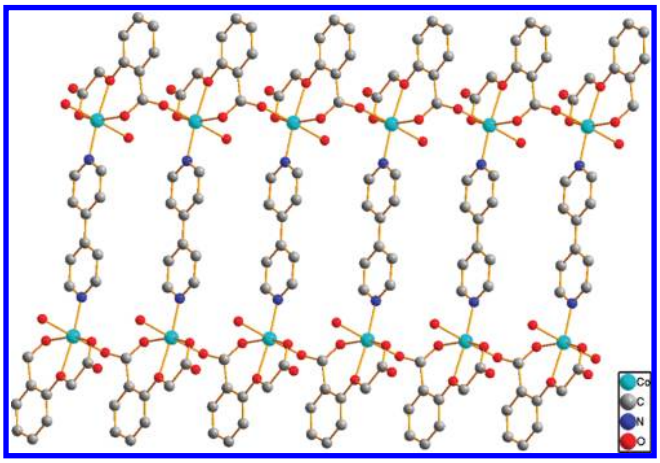

Figure 7. The 1D structure of compound **4**.

$\{[Co(OCPA)(4,4'\text{-bipy})_{1.5}]\cdot 0.5H_2O\}_n$ (5) and $\{[Ni(OCPA)(4,4'\text{-bipy})_{1.5}]\cdot 2H_2O\}_n$ (7). The structures of **5** and **7** are isomorphous with space group $P2_1/c$, and the structure of **5** was described here representatively. The asymmetric unit of compound **5** consists of one $OCPA^{2-}$, one and half a 4,4′-bipy, one Co(II) ion, and half a lattice water molecule (Figure

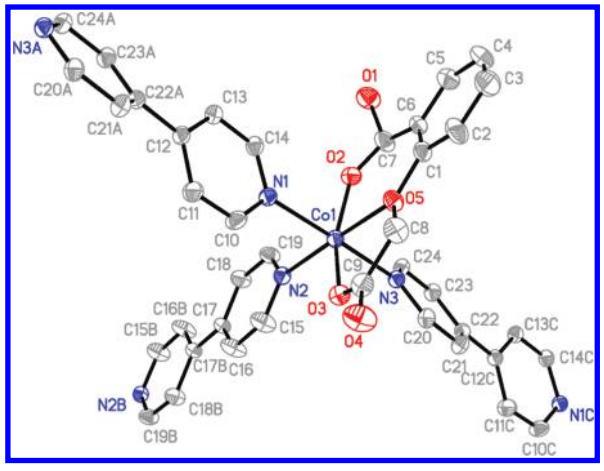

Figure 8. The molecular structure of compound **5**.

8). The hexacoordinated sphere of the Co(II) ion is completed by three nitrogen atom of three different 4,4′-bipy molecules, three oxygen atoms from one chelated $OCPA^{2-}$, resulting in a distorted CoO_3N_3 octahedral arrangement. The Co−O bond lengths range from 1.941 to 2.236 Å, and the Co−N bond distances fall in the range of 2.096−2.185 Å. In **7**, the Ni−O bond lengths range from 1.974 to 2.135 Å, and the Ni−N bond distances fall in the range 2.055−2.151 Å. Two Co(II) centers are bridged by one 4,4′-bipy molecule into a centrosymmetric binuclear unit $[Co_2(OCPA)_2(4,4'\text{-bipy})]$, and then the units bridged 4,4′-bipy molecules into an infinite 1D ladder-like chain (Figure 9), which is different from that of **4**.

$[Mn(OCPA)(H_2O)]_n$ (9). The structure of **9** belongs to the monoclinic system with chiral space group $P2_1$. The asymmetric unit of compound **9** consists of one $OCPA^{2-}$, one Mn(II) ion, and one coordinated water molecule (Figure 10). The six-coordinated sphere of the Mn(II) ion is completed by three oxygen atoms from one chelated $OCPA^{2-}$, two O_{COO}- atoms from another two $OCPA^{2-}$ and one coordinated water molecule, giving a distorted octahedron. The Mn−O bond lengths range from 2.083 to 2.390 Å. As a pentadentate ligand, each $OCPA^{2-}$ anion coordinate to three Mn(II) ions. O2, O6, and ether O1 atoms chelate to the Mn1 center, then O3 and O5 atoms link to another two Mn(II) ions. As a result, a 2D layer is formed by Mn(II) ions and $OCPA^{2-}$ anions (Figure 11).

Coordination Modes and Structural Comparison. $OCPA^{2-}$ has both rigidity and flexibility, and possesses up to five coordinated atoms, displaying rich coordination modes (Scheme 2). The tridentate coordinated mode A is observed in compounds **3**, **5**, **6**, and **7**; the tetradentate coordinated mode B exists in compounds **1**, **4**, and **8**; the pentadentate coordinated mode C appears in compound **9**; the tridentate coordinated mode D presents in compound **2**. Although both modes A and D are tridentate coordinated, $OCPA^{2-}$ ligand in mode A method chelates to one metal center, while $OCPA^{2-}$ ligand based on mode D connects two metal atoms. For the system with the same metal ions, the changes of coordination modes are driven by the different equivalents of 4,4′-bipy and trigger the giant divergence of structures among them. For Cu system, 2 equiv of 4,4′-bipy changed the coordination mode of $OCPA^{2-}$, from mode B in **1** to D in **2**, resulting in the corresponding structural transformation from 1D chain in **1** to 2D network in **2**. The number of coordinated water molecules located on the Co(II) ion in **3** is two, but only one in **4** and none in **5** (Figure 12). Because of employing 2 equiv of 4,4′-bipy as an organic base, one of two coordinated water molecules located on the Co(II) ion in **3** is replaced by the carboxyl oxygen atom, and the structure varies from a binuclear motif in **3** to a 1D chain in **4**. Interestingly, when 3 equiv of 4,4′-bipy is used, the two coordinated water molecules are completely replaced by 4,4′-bipy molecules with a structure change from a binuclear motif in **3** to a 1D chain in **5**. Compounds **6** and **7** exhibit the same rule like that of compounds **3** and **5**. But for Zn and Mn, when adjusted 4,4′-bipy from 1 to 4 equiv, the structures of both **8** (Zn) and **9** (Mn) remain unchanged. It should be noted that during the preparation the crystals of **9** could not be obtained without joining of 4,4′-bipy, although it did not emerge in the 2D network. From the above discussion, it can be concluded that the added amount of 4,4′-bipy not only can replace coordinated water molecules to form high dimension compounds (see Figure 12) but also can enhance the pH value of the synthetic environments, resulting in replacement of the water molecule by the carboxyl oxygen atoms and the change of flexible ligand configuration. Interestingly, the ladder-like structure containing 4,4′-bipy similar to **5** was reported in some research papers as molecular recognizing,[23] in which a mono- or bidentate auxiliary ligand, such as NO_3^-,[23a,c] *p*-hydroxybenzcic acid, and water,[23b] was applied.

Magnetic Properties of 1, 4, and 9. For **1**, **4**, and **9**, the comparison between powder X-ray diffraction (PXRD) and a simulated one from crystal data confirmed that the crystal phase

dx.doi.org/10.1021/cg201197k | *Cryst. Growth Des.* 2012, 12, 1201−1211

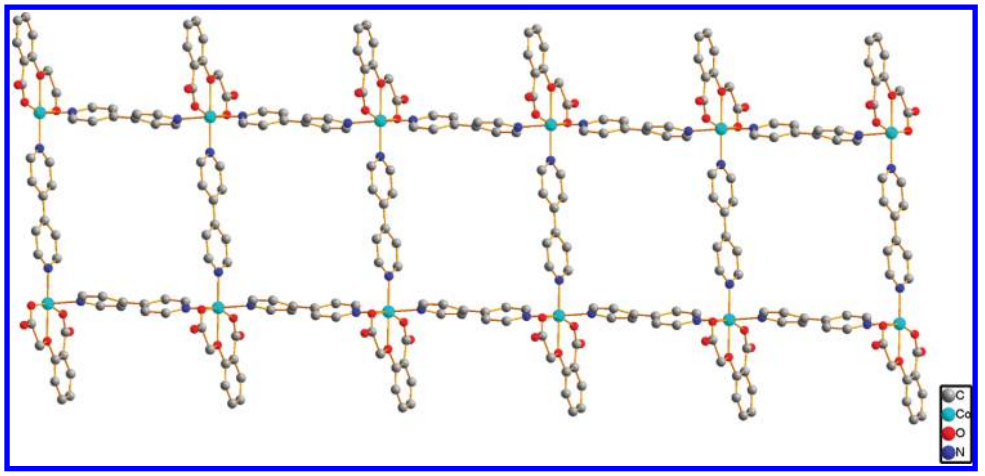

Figure 9. The 1D structure of compound **5**.

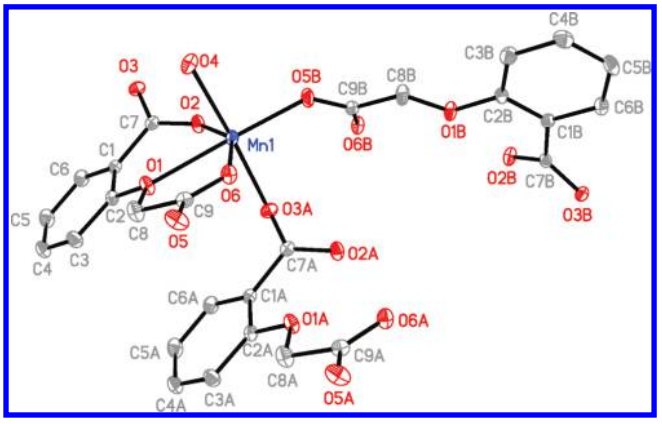

Figure 10. The molecular structure of compound **9**.

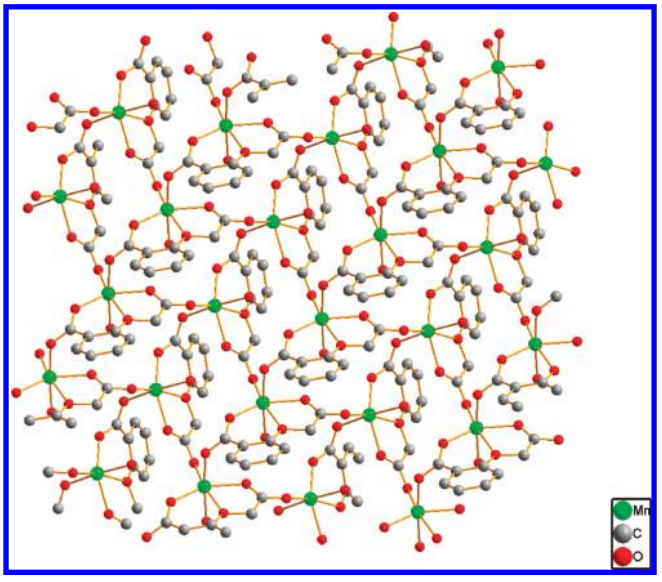

Figure 11. The 2D structure of compound **9**.

was pure (see Supporting Information). The magnetic susceptibilities of compound **1** were measured in the temperature range from 2 to 300 K and under 1000 Oe field as shown in Figure 13. The $\chi_M T$ value at 300 K is 0.371 cm^3 K mol^{-1}, which is a little lower than that expected for one Cu(II) ion (calc. 0.375 cm^3 K mol^{-1} with g = 2.0). The $\chi_M T$ value for **1** gradually decreases on cooling and reaches a value of 0.334 cm^3 K mol^{-1} at 100 K. Below 100 K, the $\chi_M T$ value sharply decreases to a value of 0.115 cm^3 K mol^{-1} at 2.0 K. The magnetic susceptibility above 30 K obeys the Curie–Weiss law with C = 0.395 cm^3 mol^{-1} K and a negative Weiss constant θ of −18.67 K (see the Supporting Information), which is smaller than that reported.[24] It is indicative of a weak antiferromagnetic interaction between adjacent Cu(II) ions in compound **1**. Because the adjacent Cu(II) ions are bridged by carboxyl groups into a 1D chain, the susceptibility data may be fitted by the Bonner–Fisher model:[9]

Scheme 2. Different Coordination Modes of OCPA^{2-} Ligand

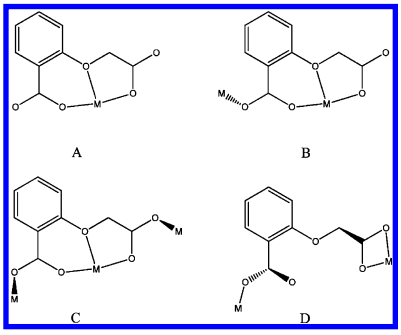

$$\chi_M = \frac{Ng^2\beta^2}{kT} \frac{0.25 + 0.074975x + 0.075235x^2}{1.0 + 0.9931x + 0.172135x^2 + 0.757825x^3}$$

$$\text{with } x = |J|/kT \quad (1)$$

Here N is Avogadro's number, β is Bohr's magneton, k is Boltzmann's constant, and J is the magnetic interaction between adjacent Cu(II) ions. The experimental data, between 30 and 300 K, could be simulated best with g = 2.04 and J = −11.07 cm^{-1}, which is a normal value in those reported for similar 1D chain antiferromagnetic copper compounds.[24] The agreement factor $R = \sum(\chi_m T_{calc} - \chi_m T_{obs})^2 / \sum(\chi_m T_{obs})^2$ is 2.05 × 10^{-4}.

The temperature dependence of the magnetic susceptibility from 2 to 300 K of compound **4** was measured under a 1000 Oe field (Figure 14). The $\chi_M T$ value at 300 K is 3.16 cm^3 K mol^{-1}, a value that is greater than that expected for a high-spin

dx.doi.org/10.1021/cg201197k | Cryst. Growth Des. 2012, 12, 1201–1211

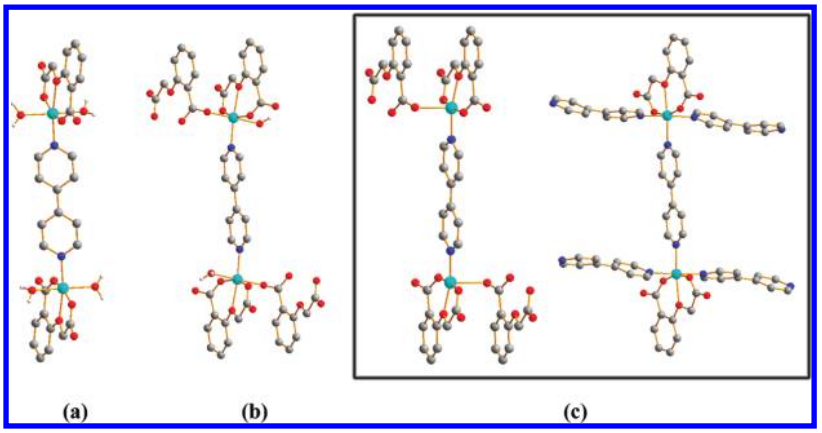

Figure 12. Different equivalents of 4,4′-bipy result in (a) two coordinated H_2O (in compounds **3** and **6**), (b) one coordinated H_2O (in compounds **4** and **8**), (c) no coordinated H_2O (in compounds **1**, **5** and **7**).

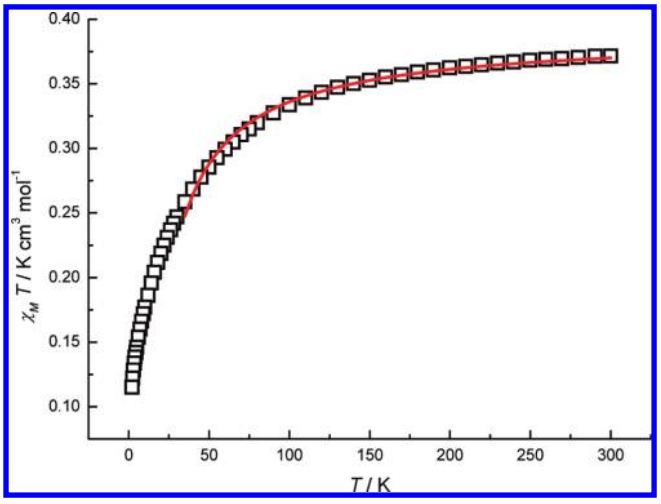

Figure 13. The plots of $\chi_M T$ versus T for **1** at 1000 Oe; the red line represents the best fit of $\chi_M T$ by eq 1 between 30 and 300 K.

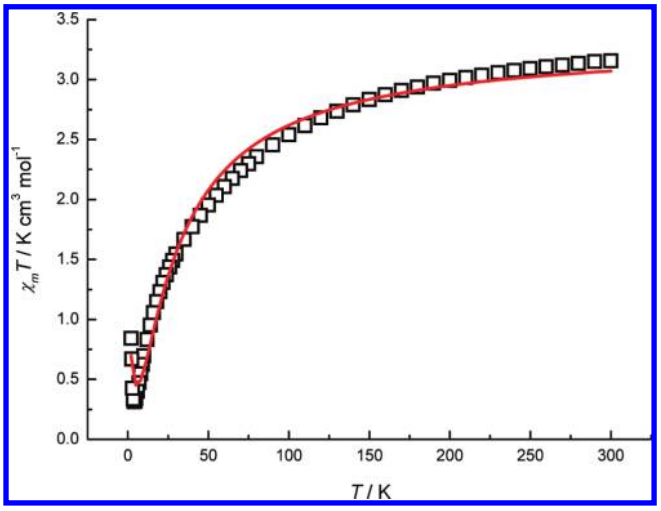

Figure 14. The plot of $\chi_M T$ versus T for **4** at 1000 Oe. The red line represents the best fit of $\chi_M T$ by eq 2.

Co(II) ion through the spin-only formula (calc. 1.88 cm^3 K mol^{-1} with g = 2.0). As the temperature decreases, the $\chi_M T$ value gradually reaches a minimum value of 0.318 cm^3 K mol^{-1} at 4.0 K. At a further decreasing temperature, the $\chi_M T$ value sharply increases to a value of 0.855 cm^3 K mol^{-1} at 2.0 K. The magnetic susceptibility above 16 K obeys the Curie−Weiss law with C = 3.59 cm^3 K mol^{-1} and a negative Weiss constant θ = −40.6 K (see Supporting Information), which might be related to both antiferromagnetic interaction and spin−orbit coupling effects for the Co(II) ion in the octahedron. The sharp increase of the $\chi_M T$ value at a low temperature is indicative of spin-canting behavior.

In the structure of **4**, the magnetic exchange interaction occurs mainly through the carboxyl bridges along the $(-OCO-Co-)_n$ chain. In order to get an estimation of the strength of the magnetic exchange interaction, it may use the following simple phenomenological equation:[25]

$$\chi T = A_1 \exp(-E_1/kT) + A_2 \exp(-E_2/kT) \quad (2)$$

Here $A_1 + A_2$ equals the Curie constant, and E_1, E_2 represent the spin−orbit coupling "activation energies" and the antiferromagnetic interaction one, respectively. The fit leads to A_1 = 3.00(5) cm^3 K mol^{-1}, A_2 = 0.32(5) cm^3 K mol^{-1}, E_1/k = 27.2(13) K, and E_2/k = −1.5(5) K (red line in Figure 14). The agreement factor R is 1.96 × 10^{-3}. The value $C = A_1 + A_2$ = 3.32(10) cm^3 K mol^{-1} is in good agreement with the Curie constant (see Supporting Information). The value E_1/k represents the effect of spin−orbit coupling, which is smaller than the reported one.[26] The value E_2 with a small exchange interaction J = −2.1 cm^{-1} ($J/k = 2E_2/k$ = −3.0 K) according to the Ising chain approximation [$\chi T \propto \exp(J/2kT)$] is close to that reported by Masciocchi and co-workers,[26] indicative of a weak antiferromagnetic interaction between Co(II) ions bridged by carboxyl groups.

To further investigate the dynamics of magnetization, alternating current (AC) magnetic susceptibilities with frequencies of 1, 10, 100, 500, 1000, and 1250 Hz were measured under H_{dc} = 0 Oe and H_{ac} = 3.5 Oe (Figure 15). The peaks of the real χ_M' and the imaginary χ_M'' parts are observed at 2.2 K. However, the peaks do not move as the frequency changes, implying that **4** is not a single-chain magnet (SCM) but is long-range ordering state with the critical temperature T_c = 2.2 K.

A plot of the temperature dependence of the field-cooled (FC) and zero-field-cooled (ZFC) measurements at an applied direct current (DC) field of 50 Oe is shown in Figure 16. The bifurcation temperature of 2.2 K is obviously observed, which is consistent with the results of AC magnetic analyses.

The magnetizations of **4** vs field were measured at 2.0 K. Below 2 kOe, it increases sharply to 0.11 $N\mu_B$ (Figure 16).

dx.doi.org/10.1021/cg201197k | Cryst. Growth Des. 2012, 12, 1201−1211

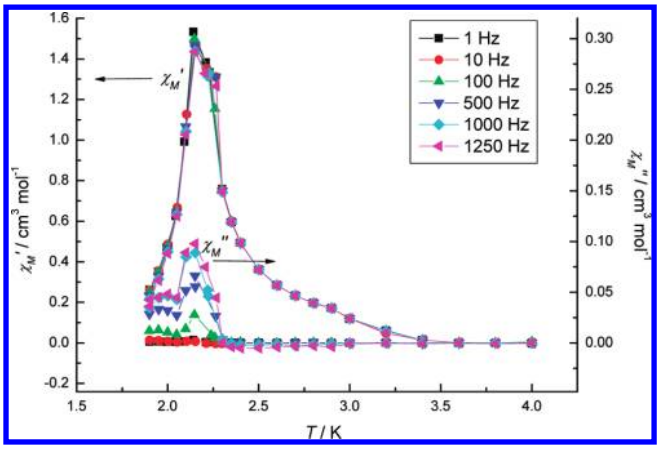

Figure 15. Temperature dependence of the in-phase and out-of-phase AC susceptibilities of **4** at the indicated frequencies, H_{ac} = 3.5 Oe and H_{dc} = 0 Oe.

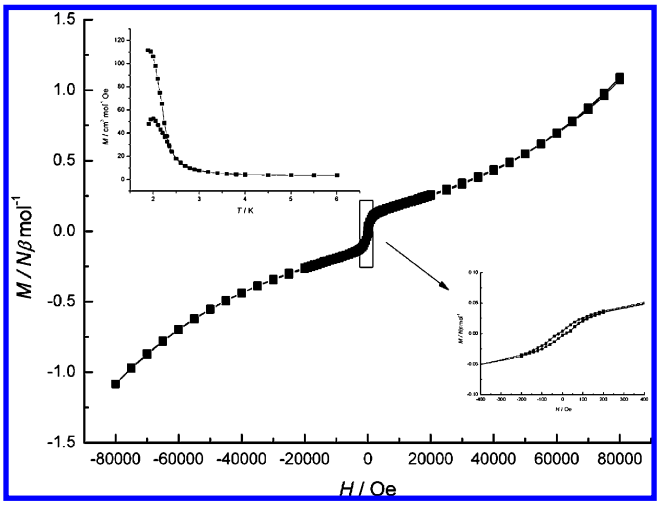

Figure 16. Field dependence of the magnetization of **4**. The right inset gives a blown-up view of the hysteresis loop below 200 Oe. The left inset shows the plots of ZFC and FC in a field of 50 Oe.

Above this field, the magnetization of **4** increases almost linearly with a small slope reaching the value of 0.43 $N\mu_B$ at 40 kOe. Up to 40 kOe, it increases with a bigger slope reaching the value of 1.1 $N\mu_B$ at 80 kOe, far lower than the experimental saturation value of the Co(II) ion, suggesting a typical spin canting magnetic behavior in **4** and antiferromagnetic coupling between Co(II) ions. A very little hysteresis loop (inset of Figure 16) is observed when the field is less than 200 Oe, giving a coercive field of 20 Oe and a very weak remnant magnetization of 0.0008 $N\mu_B$. The canting angle γ of **4** at 2 K is 1.55° which can be estimated with the equation $\sin(\gamma) = M_R/M_S$ (M_R obtained by extrapolating the high-field linear part of the magnetization curve at 2 K to zero field M_R = 0.112 $N\beta$; the total alignment of spins $M_S = gSN\beta$ = 4.15 $N\beta$, where S = 3/2 and g = 2.77 obtained through the Curie constant). The value of canting angle γ falls into a normal range, which is greater than that reported by Hong's group[10c] and smaller than that given by Gao's group.[10j]

From the results of the whole set of the experiments carried out above, it can be concluded that compound **4** is a weak ferromagnet based on antiferromagnetic interaction and spin canting with a critical ordering temperature of 2.2 K.

The magnetic properties of compound **9** were measured in the temperature range of 2−300 K at an applied field 1000 Oe, and the $\chi_M T$ vs T plots are shown in Figure 17. The $\chi_M T$ value

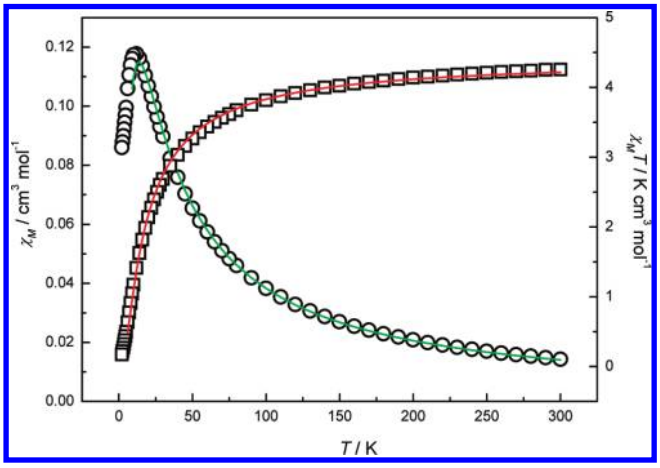

Figure 17. The plots of χ_M and $\chi_M T$ versus T for **9** at 1000 Oe. The red and green lines represent the best fit of $\chi_M T$ and χ_M according to eqs 3 and 4 above 5 K.

at 300 K is 4.26 cm^3 K mol^{-1}, close to the expected value for one Mn(II) ion (calc. 4.38 cm^3 K mol^{-1} with g = 2.0). The $\chi_M T$ value slowly decreases on cooling and reaches the value of 3.26 cm^3 K mol^{-1} at 50.0 K. As the temperature further decreases, the $\chi_M T$ sharply decreases to a value of 0.17 cm^3 K mol^{-1} at 2.0 K. The magnetic data above 20 K were well fitted by Curie−Weiss law (see Supporting Information), with the results of C = 4.56 cm^3 K mol^{-1} and a negative Weiss constant θ = −20.2 K, indicative of typical antiferromagnetic interaction between adjacent Mn(II) ions.

Taking into account the infinite 2D lattice structure of **9**, the susceptibility data were fitted by means of the Curély formula.[27] The exchange Hamiltonian $H = \sum_{nn} JS_iS_j$, where S_{nn} runs over all pairs of nearest-neighbor spins i and j (Heisenberg couplings):

$$\chi_m = [Ng^2\beta^2S(S+1)(1+u)^2]/[3kT(1-u)^2]$$
$$S = 5/2 \qquad (3)$$

Here N is Avogadro's number, β is Bohr's magneton, k is Boltzmann's constant, J is the magnetic coupling parameter between adjacent Mn(II) ions and u the Langevin function:

$$u = L(JS(S+1)/kT) = \coth(JS(S+1)/kT) - kT/JS(S+1) \quad S = 5/2 \qquad (4)$$

The best fit above 5 K leads to J = −0.86 cm^{-1} and g = 2.01 (green line in Figure 17), with $R = 5.15 \times 10^{-4}$. The negative and small J value indicates a weak antiferromagnetic coupling between neighboring Mn(II) ions, in good agreement with literature reports.[27]

Second-Order Nonlinear Optical Property of 9. Because of the chiral space group $P2_1$ of compound **9**, its second-order nonlinear optical properties were measured. A pulsed Q-switched Nd:YAG laser at a wavelength of 1064 nm was used to generate the SHG signal. The backward-scattered SHG light was collected using a spherical concave mirror and passed through a filter that transmits only 532 nm radiation. Referred to as the Kurtz powder test[28] (for more detail see

dx.doi.org/10.1021/cg201197k | Cryst. Growth Des. 2012, 12, 1201−1211

Supporting Information), the results which were obtained from a powdered sample revealed that **9** exhibited common powder SHG intensity with a response 0.8 times that of urea.[29] Notably, the Flack parameter of **9** is 0.22, which indicates that the crystal is twinning. Compared with that of an enantiopure crystal, a racemic twinning crystal structure maybe weakened the SHG response.[30]

CONCLUSION

Nine new compounds **1**–**9** were constructed based on *o*-carboxylphenoxyacetate acid ligand and under hydrothermal conditions. The different amounts of 4,4′-bipy used in the syntheses play a crucial role in tuning the structures of the compounds with the same metal ions: For Cu-containing compounds, from 1D chain **1** to 2D network **2**; for Co, through binuclear **3** to 1D ladder-like **4**, and to another different 1D ladder-like chain **5**; for Ni, from binuclear **6** to 1D chain **7**. Interestingly, for Zn and Mn, 1D chain **8** and 2D network **9** still remained unchanged under an extreme excess of 4,4′-bipy. Compound **9** with chiral space group $P2_1$ has an SHG efficiency of 0.8 times that of urea. Magnetic measurements indicate that compounds **1** and **9** have antiferromagnetic coupling between the adjacent metal ions. Importantly, compound **4** is a weak ferromagnet based on antiferromagnetic interaction and spin canting with the critical temperature T_c of 2.2 K, and it is hoped that this work provides some helpful information for future exploring the relationship between structures, weak ferromagnetism, and spin canting.

ASSOCIATED CONTENT

Supporting Information

X-ray crystallographic files in CIF format for the structure determination of compounds **1**–**9**; bond lengths and bond angles table of **1**–**9**; hydrogen bonds table and the supramolecular structures constructed by the hydrogen bonds of **3** and **6**. The plots of χ_M^{-1} versus T and PXRD of **1**, **4**, and **9**. The materials are available free of charge via the Internet at http://pubs.acs.org.

AUTHOR INFORMATION

Corresponding Author

*E-mail: zhaobin@nankai.edu.cn. Fax: +86-22-23502458.

ACKNOWLEDGMENTS

This work was supported by 973 Program (2012CB821702 and 2011CB935902), the NSFC (20971074, 91122004), FANEDD (200732), and NSF of Tianjin (10JCZDJC21700).

REFERENCES

(1) (a) Sessoli, R.; Powell, A. K. *Coord. Chem. Rev.* **2009**, *253*, 2328. (b) Kurmoo, M. *Chem. Soc. Rev.* **2009**, *38*, 1353. (c) Chen, Z.; Zhao, B.; Cheng, P.; Zhao, X. Q.; Shi, W.; Song, Y. *Inorg. Chem.* **2009**, *48*, 3493. (d) Wang, B. W.; Jiang, S. D.; Wang, X. T.; Gao, S. *Sci. China, Ser. B: Chem.* **2009**, *52*, 1739. (e) Guo, Y. N.; Xu, G. F.; Gamez, P.; Zhao, L.; Lin, S. Y.; Deng, R. P.; Tang, J. K.; Zhang, H. J. *J. Am. Chem. Soc.* **2010**, *132*, 8538.

(2) (a) Binnemans, K. *Chem. Rev.* **2009**, *109*, 4283. (b) Allendorf, M. D.; Bauer, C. A.; Bhaktaa, R. K.; Houka, R. J. T. *Chem. Soc. Rev.* **2009**, *38*, 1330. (c) Zhong, Y. W.; Vilà, N.; Henderson, J. C.; Abruña, H. D. *Inorg. Chem.* **2009**, *48*, 7080. (d) Stanley, J. M.; Zhu, X. J.; Yang, X. P.; Holliday, B. J. *Inorg. Chem.* **2010**, *49*, 2035.

(3) (a) Que, E. L.; Domaille, D. W.; Chang, C. J. *Chem. Rev.* **2008**, *108*, 1517. (b) Gunnlaugsson, T.; Stomeo, F. *Org. Biomol. Chem.* **2007**, *5*, 1999. (c) Haas, K. L.; Franz, K. J. *Chem. Rev.* **2009**, *109*, 4921. (d) Steed, J. W. *Chem. Soc. Rev.* **2009**, *38*, 506.

(4) (a) Wang, Z.; Chen, G.; Ding, K. L. *Chem. Rev.* **2009**, *109*, 322. (b) England, J.; Gondhia, R.; Bigorra-Lopez, L.; Petersen, A. R.; White, A. J. P.; Britovsek, G. J. P. *Dalton Trans.* **2009**, 5319.

(5) (a) Zhang, W.; Ye, H. Y.; Xiong, R. G. *Coord. Chem. Rev.* **2009**, *253*, 2980. (b) Zhao, H. R.; Li, D. P.; Ren, X. M.; Song, Y.; Jin, W. Q. *J. Am. Chem. Soc.* **2010**, *132*, 18.

(6) (a) Lorcy, D.; Bellec, N.; Fourmigué, M.; Avarvari, N. *Coord. Chem. Rev.* **2009**, *253*, 1398. (b) Kobayashi, Y.; Jacobs, B.; Allendorf, M. D.; Long, J. R. *Chem. Mater.* **2010**, *22*, 4120.

(7) (a) Collin, J. P.; Dietrich-Buchecker, C.; Gaviña, P.; Jimenez-Molero, M. C.; Sauvage, J. P. *Acc. Chem. Res.* **2001**, *34*, 477. (b) Jimenez-Molero, M. C.; Dietrich-Buchecker, C.; Sauvage, J. P. *Chem.—Eur. J.* **2002**, *8*, 1456. (c) Sénèque, O.; Rager, M.-N.; Giorgi, M.; Prangé, T.; Tomas, A.; Reinaud, O. *J. Am. Chem. Soc.* **2005**, *127*, 14833. (d) Skopek, K.; Hershberger, M. C.; Gladysz, J. A. *Coord. Chem. Rev.* **2007**, *251*, 1723. (e) Cavallini, M.; Bergenti, I.; Milita, S.; Ruani, G.; Salitros, I.; Qu, Z. R.; Chandrasekar, R.; Ruben, M. *Angew. Chem., Int. Ed.* **2008**, *47*, 1. (f) Gamez, P.; Costa, J. S.; Quesada, M.; Aromí, G. *Dalton Trans.* **2009**, 7845. (g) Katoh, K.; Yoshida, Y.; Yamashita, M.; Miyasaka, H.; Breedlove, B. K.; Kajiwara, T.; Takaishi, S.; Ishikawa, N.; Isshiki, H.; Zhang, Y. F.; Komeda, T.; Yamagishi, M.; Takeya, J. *J. Am. Chem. Soc.* **2009**, *131*, 9967. (h) Lang, T.; Guenet, A.; Graf, E.; Kyritsakas, N.; Hosseini, M. W. *Chem. Commun.* **2010**, *46*, 3508.

(8) (a) Wang, C. F.; Li, D. P.; Chen, X.; Li, X. M.; Li, Y. Z.; Zuo, J. L.; You, X. Z. *Chem. Commun.* **2009**, 6940. (b) Morimoto, M.; Miyasaka, H.; Yamashita, M.; Irie, M. *J. Am. Chem. Soc.* **2009**, *131*, 9823.

(9) Kahn, O. *Molecular Magnetism*; VCH: New York, 1993.

(10) (a) Rettig, S. J.; Sánchez, V.; Storr, A.; Thompson, R. C.; Trotter, J. *Dalton Trans.* **2000**, 3931. (b) Zeng, M. H.; Zhang, W. X.; Sun, X. Z.; Chen, X. M. *Angew. Chem., Int. Ed.* **2005**, *44*, 3079. (c) Yoon, J. H.; Lim, J. H.; Choi, S. W.; Kim, H. C.; Hong, C. S. *Inorg. Chem.* **2007**, *46*, 1529. (d) Chen, P. K.; Che, Y. X.; Zheng, J. M.; Batten, S. R. *Chem. Mater.* **2007**, *19*, 2162. (e) Barrios, L. A.; Ribas, J.; Arom, G. *Inorg. Chem.* **2007**, *46*, 7154. (f) Cheng, X. N.; Zhang, W. X.; Chen, X. M. *J. Am. Chem. Soc.* **2007**, *129*, 15738. (g) Li, J. R.; Yu, Q.; Tao, Y.; Bu, X. H.; Ribas, J.; Batten, S, R. *Chem. Commun.* **2007**, 2290. (h) Palii, A. V.; Reu, O. S.; Ostrovsky, S. M.; Klokishner, S. I.; Tsukerblat, B. S.; Sun, Z. M.; Mao, J. G.; Prosvirin, A. V.; Zhao, H. H.; Dunbar, K. R. *J. Am. Chem. Soc.* **2008**, *130*, 14729. (i) Marino, N.; Mastropietro, T. F.; Armentano, D.; Munno, G. D.; Doyle, R. P.; Lloretc, F.; Julve, M. *Dalton Trans.* **2008**, 5152. (j) Wang, X, Y.; Wang, Z. M.; Gao, S. *Inorg. Chem.* **2008**, *47*, 5720. (k) Duan, Z.; Zhang, Y.; Zhang, B.; Zhu, D. B. *Inorg. Chem.* **2008**, *47*, 9152. (l) Mondal, K. C.; Kostakis, G. E.; Lan, Y.; Anson, C. E.; Powell, A. K. *Inorg. Chem.* **2009**, *48*, 9205. (m) Arora, H.; Lloret, F.; Mukherjee, R. *Inorg. Chem.* **2009**, *48*, 1158. (n) Huang, F. P.; Tian, J. L.; Li, D. D.; Chen, G. J.; Gu, W.; Yan, S. P.; Liu, X.; Liao, D. Z.; Cheng, P. *CrystEngComm* **2010**, *12*, 395.

(11) Thallmair, S.; Bauer, W.; Weber, B. *Polyhedron* **2009**, *28*, 1796.

(12) (a) Gao, E. Q.; Wang, Z. M.; Yan, C. H. *Chem. Commun.* **2003**, 1748. (b) Schlueter, J. A.; Manson, J. L.; Hyzer, K. A.; Geiser, U. *Inorg. Chem.* **2004**, *43*, 4100. (c) Wang, X. Y.; Wang, L.; Wang, Z. M.; Su, G.; Gao, S. *Chem. Mater.* **2005**, *17*, 6369. (d) Cheng, X. N.; Xue, W.; Huang, J. H.; Chen, X. M. *Dalton Trans.* **2009**, 5701. (e) Clemente-León, M.; Coronado, E.; Gimenez-López, M. C.; Soriano-Portillo, A.; Waerenborgh, J. C.; Delgado, F. S.; Ruiz-Pérez, C. *Inorg. Chem.* **2008**, *47*, 9111. (f) Ko, H. H.; Lim, J. H.; Kim, H. C.; Hong, C. S. *Inorg. Chem.* **2006**, *45*, 8847. (g) Yoon, J. H.; Ryu, D. W.; Kim, H. C.; Yoon, S. W.; Suh, B. J.; Hong, C. S. *Chem.—Eur. J.* **2009**, *15*, 3661. (h) Zhang, Y.; Wang, X. T; Zhang, X. M.; Liu, T. F.; Xu, W. G.; Gao, S. *Inorg. Chem.* **2010**, *49*, 5868.

(13) (a) Li, Z. X.; Zhao, J. P.; Sañudo, E. C.; Ma, H.; Pan, Z. D.; Zeng, Y. F.; Bu, X. H. *Inorg. Chem.* **2009**, *48*, 11601. (b) Huang, F. P.; Tian, J. L.; Li, D. D.; Chen, G. J.; Gu, W.; Yan, S. P.; Liu, X.; Liao, D. Z.; Cheng, P. *Inorg. Chem.* **2010**, *49*, 2525.

(14) Gonzalez, R.; Chiozzone, R.; Kremer, C.; Munno, G. D.; Nicolo, F.; Lloret, F.; Julve, M.; Faus, J. *Inorg. Chem.* **2003**, *42*, 2512.
(15) (a) Zeng, M. H.; Yao, M. X.; Liang, H.; Zhang, W. X.; Chen, X. M. *Angew. Chem., Int. Ed.* **2007**, *46*, 1832. (b) Yao, M. X.; Zeng, M. H.; Zou, H. H.; Zhou, Y. L.; Liang, H. *Dalton Trans.* **2008**, 2428. (c) Zhou, Y. L.; Wu, M. C.; Zeng, M. H.; Liang, H. *Inorg. Chem.* **2009**, *48*, 10146. (d) Chen, Q.; Zeng, M. H.; Wei, L. Q.; Kurmoo, M. *Chem. Mater.* **2010**, *22*, 4328. (e) Chen, Q.; Zeng, M. H.; Zhou, Y. L.; Zou, H. H.; Kurmoo, M. *Chem. Mater.* **2010**, *22*, 2114.
(16) (a) Kitagawa, S.; Kitaura, R.; Noro, S. i. *Angew. Chem., Int. Ed.* **2004**, *43*, 2334. (b) Dong, B. X.; Xu, Q. *Inorg. Chem.* **2009**, *48*, 5861. (c) Fabelo, O.; Pasán, J.; Cañadillas-Delgado, L.; Delgado, F. S.; Labrador, A.; Lloret, F.; Julve, M.; Ruiz-Pérez, C. *Cryst. Growth Des.* **2008**, *8*, 3984.
(17) (a) Chen, Z.; Zhao, B.; Zhang, Y.; Shi, W.; Cheng, P. *Cryst. Growth Des.* **2008**, *8*, 2291. (b) Chen, J. Q.; Cai, Y. P.; Fang, H. C.; Zhou, Z. Y.; Zhan, X. L.; Zhao, G.; Zhang, Z. *Cryst. Growth Des.* **2009**, *9*, 1605. (c) Tzeng, B. C.; Yeh, H. T.; Chang, T. Y.; Lee, G. H. *Cryst. Growth Des.* **2009**, *9*, 2552.
(18) (a) Kirillov, A. M.; Karabach, Y. Y.; Haukka, M.; Silva, M. F. C. G. da.; Sanchiz, j.; Kopylovich, M. N.; Pombeiro, A. J. L. *Inorg. Chem.* **2008**, *47*, 162. (b) Li, C. J.; Lin, Z. J.; Peng, M. X.; Leng, J. D.; Yang, M. M.; Tong, M. L. *Chem. Commun.* **2008**, 6348. (c) Sun, W. W.; Tian, C. Y.; Jing, X. H.; Wang, Y. Q.; Gao, E. Q. *Chem. Commun.* **2009**, 4741. (d) Zheng, Y. Z.; Zhang, Y. B.; Tong, M. L.; Xue, W.; Chen, X. M. *Dalton Trans.* **2009**, 1396.
(19) (a) Kennard, C. H. L.; Smith, G.; O'Reilly, E. J. *Inorg. Chim. Acta* **1986**, *112*, 47. (b) Byriel, K. A.; Lynch, D. E.; Smith, G.; Kennard, C. H. L. *Aust. J. Chem.* **1991**, *44*, 1459. (c) Meng, F. Y.; Zhu, L. H.; Zeng, M. H.; Ng, S. W. *Acta Crystallogr. Sect. E* **2005**, *61*, 1126. (d) Yang, Y.; Meng, F. Y.; Zeng, M. H.; Ng, S. W. *Acta Crystallogr. Sect. E* **2005**, *61*, 986.
(20) (a) Hagrman, D.; Hammond, R. P.; Haushalter, R.; Zubieta, J. *Chem. Mater.* **1998**, *10*, 2091. (b) Biradha, K.; Sarkar, M.; Rajput, L. *Chem. Commun.* **2006**, 4169. (c) Liu, L.; Li, Z. F.; Wang, B. L.; Li, G.; Wang, L. P.; Meng, X. R.; He, Z. H. *Cryst. Growth Des.* **2009**, *9*, 5244. (d) Chung, H.; Barron, P. M.; Novotny, R. W.; Son, H. T.; Hu, C. H.; Choe, W. *Cryst. Growth Des.* **2009**, *9*, 3327. (e) Choi, E. Y.; Barron, P. M.; Novotny, R. W.; Son, H. T.; Hu, C. H.; Choe, W. *Inorg. Chem.* **2009**, *48*, 426.
(21) Sheldrick, G. M. *SHELXS 97, Program for the Solution of Crystal Structures*; University of Göttingen: Germany, 1997.
(22) Sheldrick, G. M. *SHELXL 97, Program for the Refinement of Crystal Structures*; University of Göttingen: Germany, 1997.
(23) (a) Losier, P.; Zaworotko, M. J. *Angew. Chem., Int. Ed.* **1996**, *35*, 2779. (b) Tong, M. L.; Chen, H. J.; Chen, X.-M. *Inorg. Chem.* **2000**, *39*, 2235. (c) McManus, G. J.; Perry, J. J.; Perry, M.; Wagner, B. D.; Zaworotko, M. J. *J. Am. Chem. Soc.* **2007**, *129*, 9094. (d) Leong, W. L.; Vittal, J. J. *Chem. Rev.* **2011**, *111*, 688.
(24) (a) Ouellette, W.; Prosvirin, A. V.; Chieffo, V.; Dunbar, K. R.; Hudson, B.; Zubieta, J. *Inorg. Chem.* **2006**, *45*, 9346. (b) Baca, S. G.; Malinovskii, S. T.; Franz, P.; Ambrus, C.; Stoeckli-Evans, H.; Gerbeleu, N.; Decurtins, S. *J. Solid State Chem.* **2004**, *177*, 2841.
(25) Rabu, P.; Rueff, J. M.; Huang, Z. L.; Angelov, S.; Souletie, J.; Drillon, M. *Polyhedron* **2001**, *20*, 1677.
(26) (a) Rueff, J. M.; Masciocchi, N.; Rabu, P.; Sironi, A.; Skoulios, A. *Eur. J. Inorg. Chem.* **2001**, 2843. (b) Rueff, J. M.; Masciocchi, N.; Rabu, P.; Sironi, A.; Skoulios, A. *Chem.—Eur. J.* **2002**, *8*, 1813.
(27) (a) Curély, J. *Physica B* **1998**, *245*, 263. (b) Curély, J. *Physica B* **1998**, *254*, 277. (c) Curély, J.; Rouch, J. *Physica B* **1998**, *254*, 298. (d) Maji, T. K.; Sain, S.; Mostafa, G.; Lu, T. H.; Ribas, J.; Monfort, M.; Chaudhuri, N. R. *Inorg. Chem.* **2003**, *42*, 709.
(28) Kurtz, S. K.; Perry, T. T. *J. Appl. Phys.* **1968**, *39*, 3798.
(29) (a) Han, L.; Hong, M. C.; Wang, R. H.; Luo, J. H.; Lin, Z. Z.; Yuan, D. Q. *Chem. Commun.* **2003**, 2580. (b) Wang, Y. T.; Fan, H. H.; Wang, H. Z.; Chen, X. M. *Inorg. Chem.* **2005**, *44*, 4148. (c) Li, X. L.; Chen, K.; Liu, Y.; Wang, Z. X.; Wang, T. W.; Zuo, J. L.; Li, Y. Z.; Wang, Y.; Zhu, J. S.; Liu, J. M.; Song, Y.; You, X. Z. *Angew. Chem.* **2007**, *119*, 6944. (d) Wen Zhang, W.; Xiong, R. G.; D. Huang., S. D. *J. Am. Chem. Soc.* **2008**, *130*, 10468. (e) Su, Z.; Chen, M. S.; Fan, J.; Chen, M.; Chen, S. S.; Luo, L.; Sun, W. Y. *CrystEngComm* **2010**, *12*, 2040.
(30) Maggard, P. A.; Kopf, A. L.; Stern, C. L.; Poeppelmeier, K. R.; Ok, K. M.; Halasyamani, P. S. *Inorg. Chem.* **2002**, *41*, 4852.